Journal of Oceanology and Limnology
Vol. 36 No. 1, P. 33-47, 2018
https://doi.org/10.1007/s00343-018-6296-5

Influences of two types of El Niño event on the Northwest Pacific and tropical Indian Ocean SST anomalies*

HU Haibo (胡海波)[1, 2, **], WU Qigang (吴其冈)[1], WU Zepeng (吴泽鹏)[1, 3]

[1] *CMA-NJU Joint Laboratory for Climate Prediction Studies, Instituted for Climate and Global Change Research, School of Atmospheric Science, Nanjing University, Nanjing 210093, China*

[2] *Key Laboratory of Meteorological Disaster of Ministry of Education, Nanjing University of Information Science and Technology, Nanjing 210044, China*

[3] *Meteorology Center of Middle South Regional Air Traffic Management Bureau of Civil Aviation of China, Guangzhou 510406, China*

Received Nov. 4, 2016; accepted in principle Dec. 20, 2016; accepted for publication Jan. 23, 2017

Abstract Based on the HadISST1 and NCEP datasets, we investigated the influences of the central Pacific El Niño event (CP-EL) and eastern Pacific El Niño event (EP-EL) on the Sea Surface Temperature (SST) anomalies of the Tropical Indian Ocean. Considering the remote effect of Indian Ocean warming, we also discussed the anticyclone anomalies over the Northwest Pacific, which is very important for the South China precipitation and East Asian climate. Results show that during the El Niño developing year of EP-EL, cold SST anomalies appear and intensify in the east of tropical Indian Ocean. At the end of that autumn, all the cold SST anomaly events lead to the Indian Ocean Dipole (IOD) events. Basin uniform warm SST anomalies exist in the Indian Ocean in the whole summer of EL decaying year for both CP- and EP-ELs. However, considering the statistical significance, more significant warm SST anomalies only appear in the North Indian Ocean among the June and August of EP-EL decaying year. For further research, EP-EL accompany with Indian Ocean Basin Warming (EPI-EL) and CP El Niño accompany with Indian Ocean Basin Warming (CPI-EL) events are classified. With the remote effects of Indian Ocean SST anomalies, the EPI- and CPI-ELs contribute quite differently to the Northwest Pacific. For the EPI-EL developing year, large-scale warm SST anomalies arise in the North Indian Ocean in May, and persist to the autumn of the El Niño decaying year. However, for the CPI-EL, weak warm SST anomalies in the North Indian Ocean maintain to the El Niño decaying spring. Because of these different SST anomalies in the North Indian Ocean, distinct zonal SST gradient, atmospheric anticyclone and precipitation anomalies emerge over the Northwest Pacific in the El Niño decaying years. Specifically, the large-scale North Indian Ocean warm SST anomalies during the EPI-EL decaying years, can persist to summer and force anomalous updrafts and rainfall over the North Indian Ocean. The atmospheric heating caused by this precipitation anomaly emulates atmospheric Kelvin waves accompanied by low level easterly anomalies over the Northwest Pacific. As a result, a zonal SST gradient with a warm anomaly in the west and a cold anomaly in the east of Northwest Pacific is generated locally. Furthermore, the atmospheric anticyclone and precipitation anomalies over the Northwest Pacific are strengthened again in the decaying summer of EPI-EL. Affected by the local Wind-Evaporation-SST (WES) positive feedback, the suppressed East Asian summer rainfall then persists to the late autumn during EPI-EL decaying year, which is much longer than that of CPI-EL.

Keyword: EPI-EL; CPI-EL; Indian Ocean SST anomalies; zonal SST gradient in the Northwest Pacific; Northwest Pacific anticyclone anomaly; East Asian Summer rainfall

1 INTRODUCTION

El Niño event (EL) is the most significant phenomenon of interannual variability in the climate system, and plays an important role in the global climate anomalies (Zhang, 1999). The spatial

* Supported by the National Key Program for Developing Basic Science of China (Nos. 2012CB956002, 2016YFA0600303), the National Natural Science Foundation of China (Nos. 41675064, 41621005, 41330420, 41275068), the Jiangsu Province Science Foundation (No. SBK2015020577), and the Jiangsu Collaborative Innovation Center of Climate Change and Key Laboratory Project Foundation (No. KLME1501)
** Corresponding author: huhaibo@nju.edu.cn

distribution of Sea Surface Temperature (SST) anomalies for the traditional EL is consistence with the first EOF mode of SST anomalies in the tropical Pacific Ocean (McPhaden et al., 1998; Wallace et al., 1998). The SST anomaly generally appears in the summer and autumn of the EL developing year, reaches its peak in the winter and decays quickly in the summer of the EL decaying year. Accompany with the development of EL, two types of significant Sea Surface Temperature (SST) interannual variability events exist in the tropical Indian Ocean, which are named as Indian Ocean Basin Mode (IOB) and Indian Ocean Dipole (IOD) mode (Saji et al., 1999; Du et al., 2009; Xiao, 2009; Xie et al., 2009). There is a close relation between various SST anomalies in the two basins, and this relationship is more obvious in the last few decades (Huang et al., 2010; Guo et al., 2015). Along with the evolution of these SST modes, the East Asian summer monsoon and summer precipitation over East Asia have significant annual variation. According to Wang et al. (2000), Xie et al. (2009) and Fan et al. (2013), the interannual variability of East Asian summer monsoon is related to the tropical SST interannual anomaly mode, through the interannual variability of the Northwest Pacific cyclonic (anticyclonic) atmospheric circulation.

The positive IOB anomaly usually occurs three months after the traditional EL. The warm SST anomaly maintains until next summer though the positive SST anomaly in the tropical Middle East Pacific Ocean has disappeared (Klein et al., 1999; Yang et al., 2007; Xie et al., 2009; Du et al., 2011). Du et al. (2009) pointed out that in a traditional EL, affected by the westward propagating sinking ocean Rossby waves, warm SST anomaly first appeared in the Southwest Indian Ocean. It inspires "C-type" wind anomaly wind in the tropical Indian Ocean basin. When the South Asian summer southwest monsoon onset, due to the reduction of upward latent heat over North Indian Ocean, warm SST anomalies exist over the entire Indian Ocean. But IOB event do not always occurs after each EL (Hu et al., 2011). In addition, EL may influence the occurrence of the IOD event (Murtugudde et al., 2000; Annamalai et al., 2003; Nagura and Konda, 2007; Roxy et al., 2011). When the typical EL occurs, a coupled mode with independent variability in the equatorial East India Ocean is strengthened. The corresponding wind anomalies thereby have influences on the East India Ocean SST and may lead to an IOD event. Conversely, the tropical India Ocean SST anomaly have influences on the Pacific SST anomaly. In the "India-Pacific gear" theory (GIP) proposed by Wu and Meng (1998), the mesh point of GIP first appeared in India ocean, and then gradually spread eastward to the Pacific. Through a coupled model, Wu and Kirtman (2004) showed that the ENSO variability was significantly reduced excluding the air-sea coupling in Indian Ocean. Tan et al. (2004) found that the development of SST anomalies from IOB to IOD in Indian Ocean corresponds to the development of a traditional EL. Zhao and Yang (2004) found that tropical Indian Ocean SST anomalies always lead to the anti-phase changes of tropical Pacific SST anomaly by the action of wind stress bridge on both interannual and decadal time scales.

Xie et al. (2009) found that the interannual variability of Indian Ocean SST anomaly had influences on the atmospheric deep convection, and then excited the eastward baroclinic Kelvin wave accompanied with significant east wind anomaly. According to Ekman divergence mechanism, the easterly wind anomaly results in anomalous down-welling over Northwest Pacific, which suppresses atmospheric convection and leads to a low-level anomalous anticyclone over Northwest Pacific. Wang et al. (2000) proved that the low-level anticyclonic anomaly could also be excited by the local negative SST anomaly in Northwest Pacific. According to local Wind-Evaporation-SST (WES) (Xie and Philander, 1994) positive feedback, Hu et al. (2011) further pointed out that during the summer of EL decaying year, the zonal SST anomaly gradient in Northwest Pacific was conducive to the maintenance of the Northwest Pacific anticyclone. By using an AGCM, Annamalai et al. (2005) proved that the warm Indian Ocean SST anomaly led to easterly wind anomaly in the tropical western Pacific and anticyclonic circulation anomaly over Northwest Pacific. Hu et al. (2013a, b) illustrated the contribution of the IOB warming to the maintenance and enhancement of the Northwest Pacific anticyclone in the summer of EL decaying year, and stressed the importance of the outbreak of the South Asian Summer Monsoon.

In recent decades, the geographical locations of SST anomaly during the ELs have changed dramatically. More and more Central-Pacific-ENSO (Yu and Kao, 2007; Kao and Yu, 2009; Yeh et al., 2009), Warm-Pool-ENSO (Kug et al., 2009) and the ENSO-Modoki events appear in the tropical Pacific (Ashok, 2007). Back in the 1980s, Fu and Fletcher (1985) found that two types of EL exist in the eastern

and central equatorial Pacific, respectively. Choi et al. (2012) and McPhaden et al. (2011) put forward that the migration of ENSO is related to two types of SST subsurface spatial modes (the ENSO-Induced-TPDV and ENSO-Like-TPDV) over Pacific Ocean. Distinguish from the "eastern type" EL (EP-EL), which has warm SST anomaly in tropical East Pacific Ocean (Rasmusson and Carpenter, 1982; Kao and Yu, 2007), the so-called "central type" EL (CP-EL) refers to the frequent occurrence of interannual SST anomaly warming event in the equatorial central Pacific Ocean (even extend west to the Nino-4 region) (Yu and Kao, 2007; Kao and Yu, 2009). In previous studies, a variety of index and classification method on these two types of EL have been defined (Trenberth and Tepaniak, 2001; Larkin and Harrison, 2005; Ashok et al., 2007; Peng et al., 2011; Ren and Jin, 2011; Yu and Kim, 2011; Zhang et al., 2011). Although the dynamic mechanism of CP-EL is still unclear, some observations have shown that, the positions of SST anomaly in EP- and CP-ELs are quite different. So the influences of two types of EL on global and East Asian climate have significant difference (Weng et al., 2007; Yeh et al., 2009; Feng and Li, 2011; Weng et al., 2011; Xu et al., 2012; Wang and Wang, 2013). Especially, different effects of the two types of EL have been found on the Northwest Pacific anticyclone (Feng, 2010, 2011; Feng and Li, 2011; Yuan et al., 2012). Zhang et al. (2011) further contrasted the effects of two types of EL on the atmospheric circulation over Northwest Pacific. The results indicated different effects of these two types of EL on East Asian climate, especially the South China precipitation.

Previous studies have proved that for traditional definition of ENSO (or EP-EL), there is a significant relationship between EL and the SST interannual variation in the Indian Ocean. Wang and Wang (2013a, b) and Wang et al. (2014) put forward that the traditional EL and two types of Modoki EL events have different effects on the development of IOD event and the autumn rainfall anomaly distribution of China. But there are few studies on the impacts of two types of EL (EP and CP) on the Indian Ocean basin during the EL developing and decaying years. According to Xie et al. (2009) and Hu et al. (2013b), the Indian Ocean consistency warming event has an important influence on the Northwest Pacific anticyclone and the East Asian summer rainfall in the summer of the EL decaying year. Considering the classification of two types of ELs, this paper will mainly discuss the different responses of two types of interannual SST anomaly mode in tropical Indian Ocean for EL developing and decaying years and the influences of these Indian Ocean SST anomaly modes on the Northwest Pacific.

2 DATA AND METHOD

2.1 Data

In this paper, the data sets include: 1) Hadley Centre Sea Surface Temperature dataset (HadISST1), which is a unique combination of monthly globally-complete fields of SST on a 1-degree latitude-longitude grid from 1950/01 to 2016/10; 2) The National Centers for Environmental Prediction (NCEP) Reanalysis dataset, which has 2.5-degree latitude-longitude global grid from 1950/01 to 2016/10, including wind and precipitation.

In this paper, we first remove the seasonal cycle and long-term trend to get the interannual variability. In order to get the two distribution patterns of EL, we used the method in Kao and Yu (2009) (but the long-term trend have been removed), to classify the interannual SST anomalies in the equatorial Pacific between 1950 and 2006. First of all, the equatorial Pacific is divided into the Niño 1+2 region (80°–90°W, 10°S–0°), Niño 3 region (150°–90°W, 5°S–5°N), Niño 3.4 region (170°–120°W, 5°S–5°N) and Niño 4 region (160°–150°W, 5°S–5°N). Then the Niño 1+2 index is subtracted from the prior equatorial SST anomalies before the EOF analysis, to obtain the CP-EL. Similarly, the leading structure of the SST anomalies in EP-EL is obtained by subtracting the Niño 4 index before the EOF analysis. By regressed the time series of these two EOF modes to the sea surface wind, we get the distributions of the sea surface wind interannual anomaly which are related to EP- and CP-ELs (Fig.1). Similar as the result of Kao and Yu (2009), EP- and CP-ELs respectively explain about 30% of the total interannual variance (long-term linear regression has been removed). The SST anomalies of EP-EL located in Niño 1+2 and Niño 3 regions, and spread narrowly in meridional direction. However, the SST anomalies of CP-EL occupy the tropical East Pacific and the subtropical Pacific. Especially in the Northeast tropical Pacific of CP-EL, the SST anomaly also reaches the same order of magnitude in the Niño 4 region. Unlike the meridional symmetry distribution of SST anomaly, the sea surface wind anomalies of EP-EL show meridional asymmetry obviously. The northward

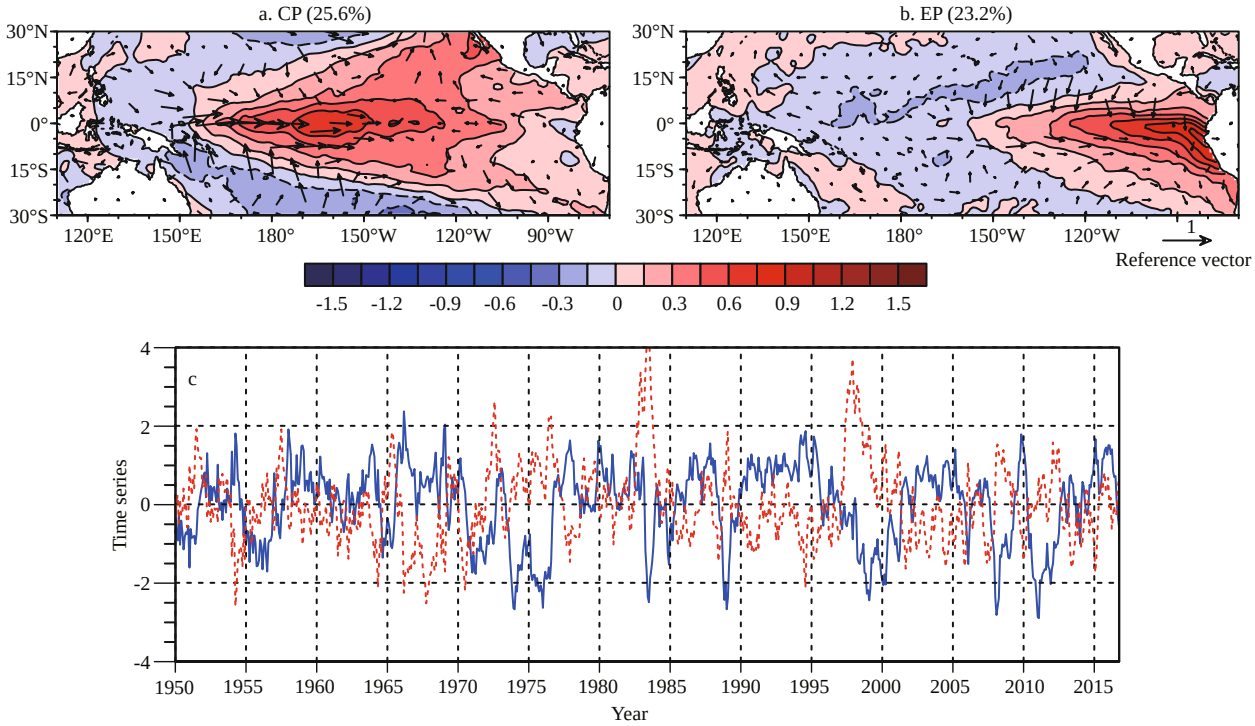

Fig.1 CP- (a), and EP-ELs (b) and the spatial distribution of their SST anomaly (with the corresponding sea surface wind anomalies) and their time series (c)

Spatial mode contour interval is 0.5°C, blue solid lines are corresponding time series for CP -EL and red dotted lines are for EP-EL. The sea surface wind is the regression value that passes the reliability test.

wind over the South Pacific is obviously stronger than that in the north of the equator (Fig.1b). The interannual sea surface wind anomalies for CP-EL are obvious different. With the maximum of the SST anomalies as the position center for CP-EL, westerly wind anomaly persists in the west (the strongest equatorial westerly anomalies located between 160°E and 180°E), while, the easterly anomalies exist in the east. Off the equator, significant wind convergence appears towards the SST anomaly. In addition, along with the wide range of meridional SST anomaly in the CP-EL, there is a cyclonic circulation anomaly over the warm SST in the Northwest subtropical Pacific (Fig.1a). The EP- and CP-ELs have different spatial distributions and time series. As Fig.1c shows, there are several strong ELs in the time series of EP-EL, while strong La Niña events are more pronounced in the CP -EL.

In order to better reflect the impact of EL on the India Ocean SST anomalies, we further screened typical events by setting the threshold of ENSO episodes as the time series exceeding its 0.75 standard deviation for 5 consecutive months. The relationship between the consecutive strong ENSO event and India Ocean SST anomaly is more closely (Xie et al., 2009; Hu et al., 2011). Accordingly, we get 9 (EP) and 17 (CP) strong El Niño cases (Table 1), while 15 (EP) and 8 (CP) strong La Niña events, respectively. Figure

Table 1 The cases of EP- and CP-ELs

EP–EL	CP–EL
195106–195112	195711–195803
195703–195712	195810–195902
196502–196601	196307–196402
197205–197301	196509–196612
197605–197612	196810–196902
198208–198312	197708–197804
199705–199808	198706–198801
200712–200809	199007–199101
201112–201207	199110–199203
	199212–199306
	199312–199411
	199412–199506
	200212–200304
	200312–200410
	200909–201003
	201412–201504
	201508–201605

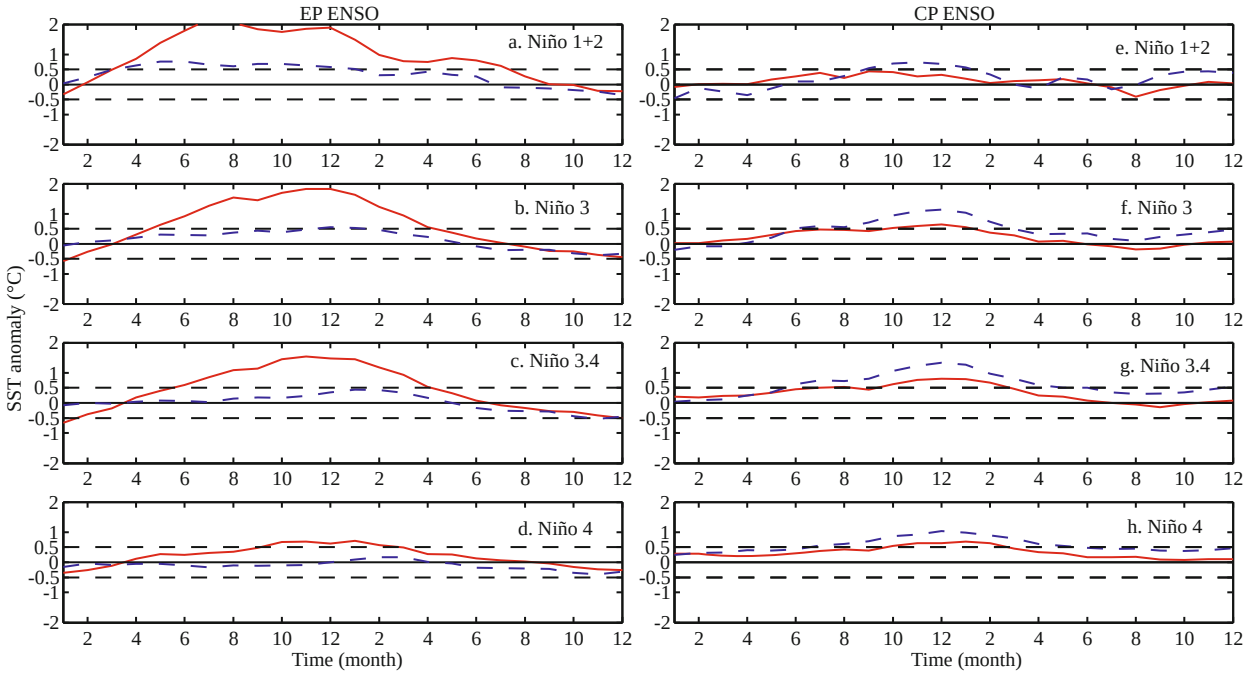

Fig.2 Composites of Niño SST indices for the warm (red solid lines) and cold (blue dashed lines) phases of the EP- (a–d) and CP-ELs (e–h)

2 shows the composite Niño SST indexes for the El Niño and La Niña phases of two types of ENSO, with continuous seasonal evolution. Under the definition of abnormal events in this paper, it can also be found that the tropical Pacific SST anomaly first appears in the Niño 1+2 region for EP-EL (in the developing year summer), then propagates west in winter of the developing year and reaches its peak (Fig.2). The SST anomaly intensity for EP-EL is stronger than that in EP type La Niña. However, the SST anomaly for CP-EL maintains in the middle tropical Pacific for the whole life cycle and reaches its peak in winter of developing year (Fig.2). On the whole, the strength of the CP type La Niña event is greater than that of El Niño event. For the discontinuous CP-EL SST anomalies events, they cannot provide persistent impacts on the Indian Ocean and are not taken into consideration.

3 THE DISTRIBUTION OF THE INDIAN OCEAN SST ANOMALY AND THE NORTHWEST PACIFIC PRECIPITATION ANOMALY UNDER THE TWO TYPES OF EL

3.1 Effects of two types of EL on the India Ocean SST anomaly

In order to get the effects of these two types of EL on the Indian Ocean, the sea surface temperature and sea surface wind anomalies of these two types of EL from August to November (Aug(0)–Nov(0)) of the EL developing year, and from June to September (Jun(1)–Sep(1)) of the decaying year were composited, separately (Fig.3 and Fig.5). As shown in Fig.3, the SST anomalies in tropical Indian Ocean were obviously accompanied with the warm SST anomalies in the middle-east tropical Pacific. The obvious SST anomalies of IOD positive phase (a warm anomaly in the west and a cold anomaly in the east) in EP-EL persisted from Aug(0) to Nov(0), while only weak warm SST anomalies existed in CP-EL.

In order to reflect the influences of the two types of EL on the development of the Indian IOD events, we selected the western tropical Indian Ocean (50°–70°E, 10°S–10°N) and eastern tropical Indian Ocean (90°–110°E, 10°S–0°) as the representative positions (Xiao et al., 2009). The IOD index was defined as:

$$IOD=SSTA_W–SSTA_E. \quad (1)$$

Among them, $SSTA_W$ and $SSTA_E$ respectively represented the west and east tropical Indian SST anomaly in the Fig.4. There was almost no zonal temperature gradient in tropical Indian Ocean in the CP-EL developing year. However, the IOD index of the EP-EL began to develop rapidly in late summer, and reached its peak in autumn, but declined rapidly in winter. In developing year of CP-EL, weak SST anomalies of positive IOD index persisted in tropical India Ocean for only one month.

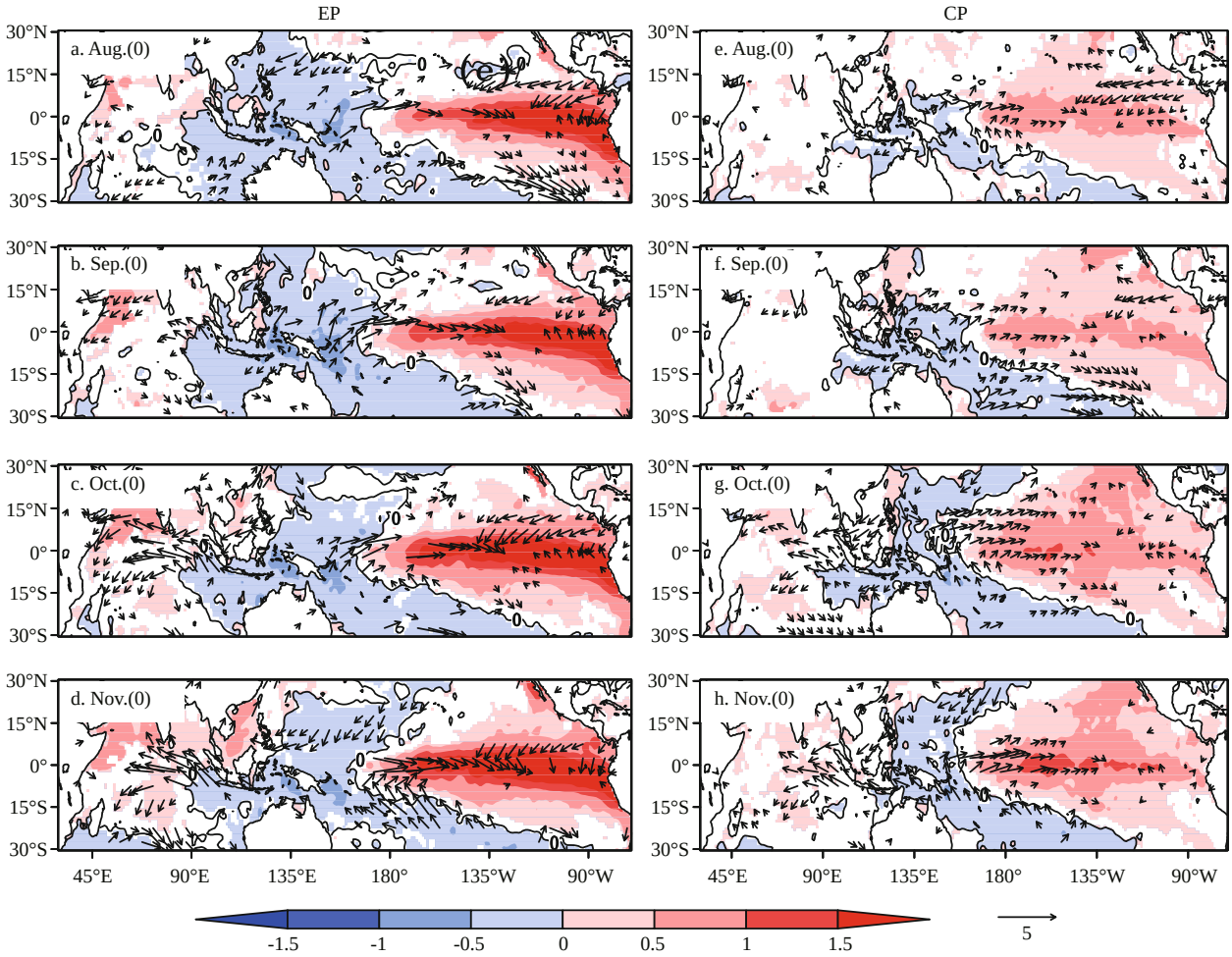

Fig.3 Composites of SST and surface winds anomalies in the developing year of (a–d) EP- and (e–h) CP-ELs are showed from August to November

Wind vectors and SST (shaded) are shown when they pass the 95% Student's *t* significance test. Black solid lines denote the zero contour lines.

Similar to Zhang et al. (2011), along with the seasonal evolution of SST anomaly of IOD events, the composite sea surface wind anomalies in Fig.3 showed that there were significant easterly anomalies over the tropical East Indian Ocean, while westerly anomalies over the tropical West Indian Ocean in the autumn of EP-EL developing year. However, among Aug(0) and Sep(0) of CP-EL developing year, there were no obvious SST or wind anomalies in the whole tropical Indian Ocean. Due to the presence of the cold SST anomaly in the October of CP-EL in tropical East Indian Ocean, the tropical Indian Ocean also had weak easterly anomalies similar to that of EP-EL. In addition, westerly anomalies over the Northwest Pacific in CP-EL were significantly stronger than that in autumn of EP-EL developing year. Murtugudde et al. (2000) pointed out that IOD events might be caused by the ocean-atmosphere interaction only in the Indian Ocean, and it could not be strengthened

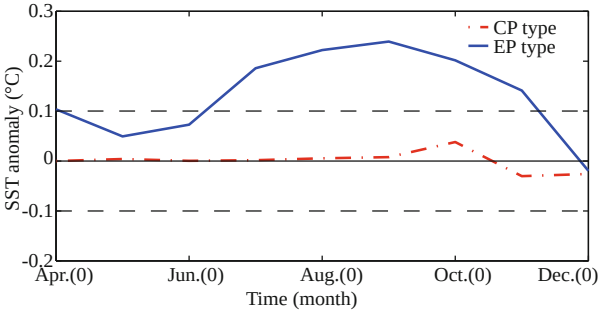

Fig.4 Time series of IOD index in the developing year of EP- (blue solid lines) and CP-ELs (red dashed lines)

Units: °C. Black dashed lines denote the ±0.1°C lines.

during an EL. So there was a coupled mode with its own variability in equatorial Indian Ocean, with the cold SST anomaly in the equatorial East Indian Ocean in the autumn season. However, in the fall of EP-EL developing year, due to the forcing of the equatorial Pacific warm SST anomaly, the equatorial East Indian

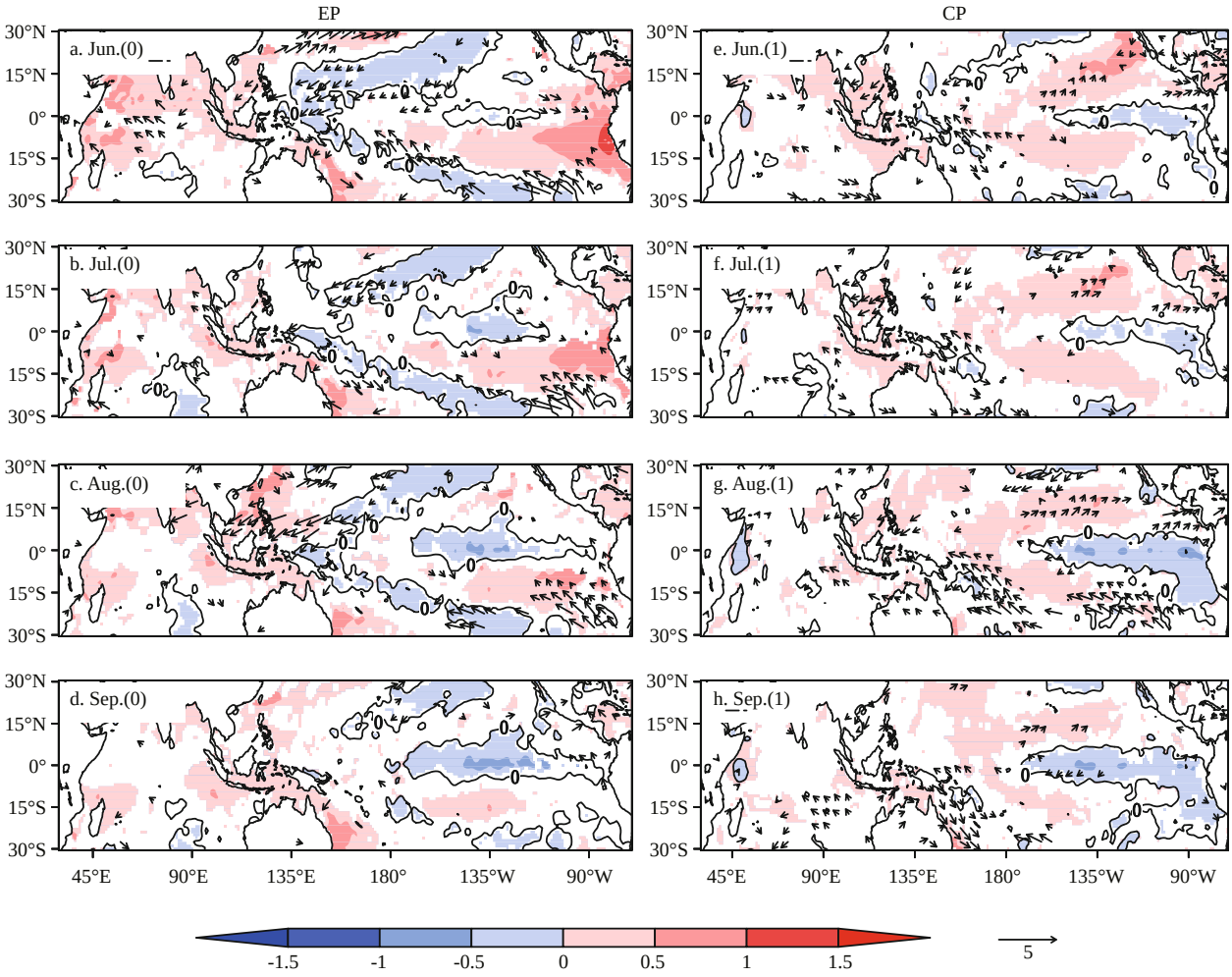

Fig.5 Composites of SST and surface winds anomalies of EP-EL from (a–d) June to September and (e–h) anomalies of the CP-EL

SST anomalies are shaded and wind vectors are shown when they pass the 95% Student's t significance test. Black solid lines denote the zero contour lines of SST anomaly.

Ocean cold SST anomaly developed rapidly and also led to IOD event ultimately. At the same time, the existence of IOD positive phase SST anomaly might strengthen the westerly anomaly over the tropical West Pacific. Annamalai et al. (2005) using the numerical experiments proved that the positive IOD SST anomaly caused a significant downdraft over the cold SST anomaly in tropical East Indian Ocean. So easterly sea surface wind anomalies existed to the west of the downdraft, but westerly anomalies over the tropical west Pacific lower. The westerly anomalies favored warm SST anomaly in the tropical east Pacific by the warm water advection and the eastward propagation of the oceanic sinking Kevin wave. This may be the reason why the EP-EL warm SST anomaly is stronger (Fig.3).

In the decaying year of EL, the Indian Ocean has a "capacitor" effect (Yang et al., 2007). At this time, equatorial Middle East Pacific SST anomaly almost disappeared, but the Indian Ocean basin warming anomaly still existed, even persisted to the summer, and prolonged the effects of El Niño event on the global climate. Xie et al. (2009) and Hu et al. (2011) demonstrated that the Indian Ocean basin consistency warming after traditional EL has an important impact on the Northwest anticyclonic atmospheric circulation and the summer rainfall in the East Asia. Figure 5 shows the evolution characteristics of SST and sea surface wind anomalies in the Indian-Pacific basin in the decaying summer of two types of EL. In the decaying summer, warm SST anomalies in the tropical Middle East Pacific are significantly weakened for both ELs. After the August of EL decaying year, the equatorial Middle East Pacific generates cold SST anomaly, which represents the rapid decline of EL. At the same time, basin uniform warm SST anomalies

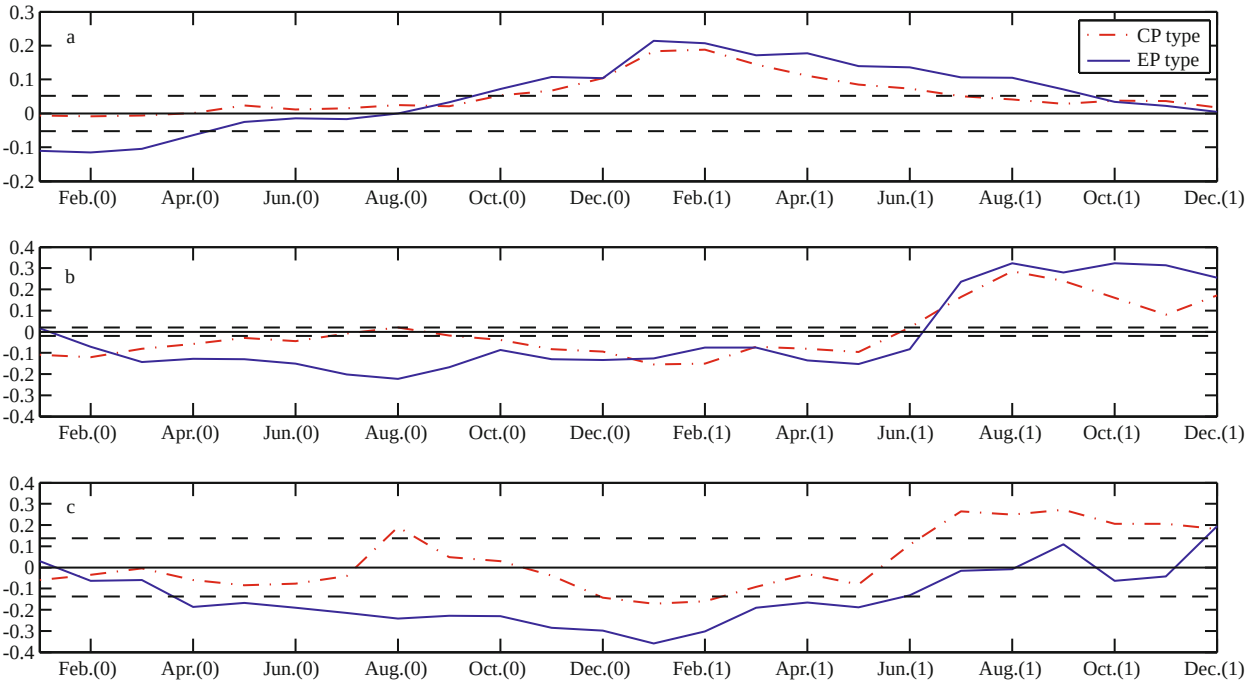

Fig.6 (a) Time evolutions of the IOB index for EP- and CP-ELs; time evolutions of the SST anomalies in the Northwest Pacific (b) west region (125°–145°E,4°–20°N) and (c) east region (145°–170°E, 4°–20°N) during the two types of EL

The blue solid lines denote the composites of SST anomalies in the EP-EL and the red dashed lines denote the SST anomaly composites in the CP-EL. Unit: °C.

exist in the Indian Ocean in the whole summer of EL decaying year for both CP- and EP-ELs. However, considering the significance, more significant warm SST anomalies only appear in the North Indian Ocean among the June and August of EP-EL decaying year. Another significant difference between EP- and CP-ELs is manifested in the Northwest Pacific. For the EP-EL, the Northwest Pacific cold SST anomaly persists to the autumn of decaying year with eastward shrinking. However, after the June of the CP-EL decaying year, the entire Northwest Pacific shows a weak warm SST anomaly. Accompany with the different zonal SST gradient between the tropical Indian Ocean and Northwest Pacific, the sea surface wind anomalies over Northwest Pacific show significant differences for the two types of EL. Significant northeasterly wind anomaly appears in the EP-EL decaying summer, which is almost invisible in the same period of CP-EL.

In order to clearly compare the difference of the Indian Ocean summer SST anomaly between the two types of EL decaying year, Fig.6 shows the evolution characteristics of the average SST anomaly in the tropical Indian Ocean (the IOB index from Du et al. (2009)). As can be seen from the figure, the Indian Ocean warming developed slowly and declined rapidly for CP-EL developing summer. While for EP-EL, the tropical Indian Ocean warming developed rapidly in Aug(0) and maintained the significant positive SST anomaly. At the same time, the Northwest Pacific can be divided into the eastern and western regions by different SST anomaly evolution characteristics for EP- and CP-ELs (Fig.6b, c). Among them, similar evolution characteristics exist in the western region of Northwest Pacific for both ELs (Fig.6b). However, the variations of SST anomaly in the Northwest Pacific eastern region are markedly different between EP- and CP-ELs. In the CP-EL, a weak cold SST anomaly exists in the Northwest Pacific from the EL developing year but quickly turns into positive anomaly in the June of EL decaying year (Fig.6c). However, the cold SST anomaly in the eastern Northwest Pacific persists until the August of CP-EL decaying year. Fan et al. (2013) pointed that this cold SST anomaly was crucial in the developing and maintaining the Northwest Pacific cyclonic (anticyclonic) atmospheric circulation during the East Asian Summer Monsoon.

In the autumn of the EP-EL developing year, it's conducive to the development of the equatorial East Indian Ocean cold SST anomaly, and eventually leads to the IOD event. Besides, the presence of IOD positive

SST anomaly during the autumn of EP-EL developing year, in turn enhances the westerly wind anomaly over the west tropical Pacific westerly, and possibly strengthens the EP-EL warm SST anomaly through the ocean warm advection and the eastward Kelvin wave. This may be one reason why warm SST anomaly in EP-EL is stronger than that in CP-EL. For the EL decaying year, the tropical Indian Ocean shows basin consistency warming (IOB) and it maintains until the EL decaying year for both types of EL. In the case of CP-EL, IOB warming is earlier, but weaker than that of EP-EL in the decaying summer. It may be associated with the strength of the equatorial Pacific SST anomaly for two types of EL. Similar differences are also reflected in the distribution of the SST anomalies in the Northwest Pacific in summer of two types of EL decaying year. Wang et al. (2000) proposed that the Northwest Pacific cold SST anomaly remained in the Northwest Pacific from the EL developing year, suppressed the local atmospheric convective activity, and strengthened the local anticyclonic atmospheric circulation anomalies. So more latent heat flux released from ocean, and led to the local cold SST anomaly, which established a positive feedback between Northwest Pacific anticyclonic atmospheric circulation anomalies and local cold SST anomalies. Another negative feedback was proposed by Wu et al. (2010) and Hu et al. (2011), that the Northwest Pacific atmospheric circulation anomalies anticyclonic suppressed local convection and cloud cover, which was beneficial for more shortwave radiation and increasing of local sea surface temperature. In addition, the tropical Indian Ocean warming is favorable to the maintenance of cold SST anomaly in the Northwest Pacific by stimulating the atmospheric Kelvin waves, which leads to significant northwesterly and increases the release of latent heat to the atmosphere (Xie et al., 2009; Hu et al., 2013b). In two types of EL, cold SST anomaly appears in the Northwest Pacific west region, but quickly turns into warm SST anomaly in late spring of EL decaying year. However, the cold SST anomaly in Northwest Pacific east region could maintain to the EL decaying summer.

3.2 The impacts of Indian Ocean basin warming abnormal on Northwest Pacific under the two types of EL

Results above showed that the two types of EL are conducive to Indian Ocean warming and Northwest Pacific cooling. Previous works showed that both local cold SST anomaly in Northwest Pacific along with the emergence of EL (Wang et al., 2000) and the warm SST anomaly in Indian Ocean may lead to Northwest Pacific anticyclonic atmospheric circulation anomalies (Xie et al., 2009). In order to better distinguish the differences of Indian Ocean SST anomalies with different types of EL, especially the different effects on the Northwest Pacific, we selected those cases that the Indian Ocean continuous and significant warming in EL decaying year (Indian Ocean SST anomaly exceeding the 0.75 standard deviation of IOB time series for 5 consecutive months; Hu et al., 2011) from the existing EP- and CP-ELs. They are defined as EPI (EP-IOB, 6 cases) and CPI (CP-IOB, 4 cases), respectively. Figure 7c shows the characteristics of IOB index in EL evolution process for the EPI and CPI events. As shown in the figure, in CPI-EL, the Indian Ocean warm SST anomaly is weak, maintains for a short time from the winter of developing year to the next late spring. The maximum of Indian Ocean warm SST anomaly in EPI-EL is eight times than that of CPI-EL. Besides, the Indian Ocean warm SST anomaly in EPI-EL persists from the late spring of EL developing year to the late autumn of decaying year. This difference of SST anomaly in the South Indian Ocean is especially evident (Fig.7b). Du et al. (2011) pointed out that the warm SST anomaly in north Indian Ocean is most pronounced with IOB Warming event during EL decaying year, and has a notable impact on Northwest Pacific. Under the classification of two types of EL in this paper, the North Indian Ocean warm SST anomaly in CPI-EL lasts from May(0) to Jul(1). For the case of EPI-EL, it begins in May(0), reaches its peak (nearly 0.3°C) in developing winter, and decays rapidly after Aug(1). Thus, in EPI-EL, the sustained North Indian Ocean warming is more remarkable and the North Indian Ocean keep warm SST anomaly until the autumn of EL decaying year. In CPI-EL, however, the warm SST anomaly is weak and stays until Jul(1).

Similar to Figs.7, 8, 9 show the differences of SST, wind and rainfall anomalies between CPI- and EPI-ELs in the summer of decaying year, respectively. In the summer of EPI-EL decaying year, subtropical Northwest Pacific maintains significant zonal SST gradient, with a wide range of continuing warm SST anomaly (purple contour region in Fig.8) in the west of 145°E including the South China Sea and a wide range of negative SST anomaly (green contour region) to the east of 145°E. Over this zonal SST gradient region, there are anticyclonic atmospheric circulation anomalies. In the August of EPI-EL decaying year,

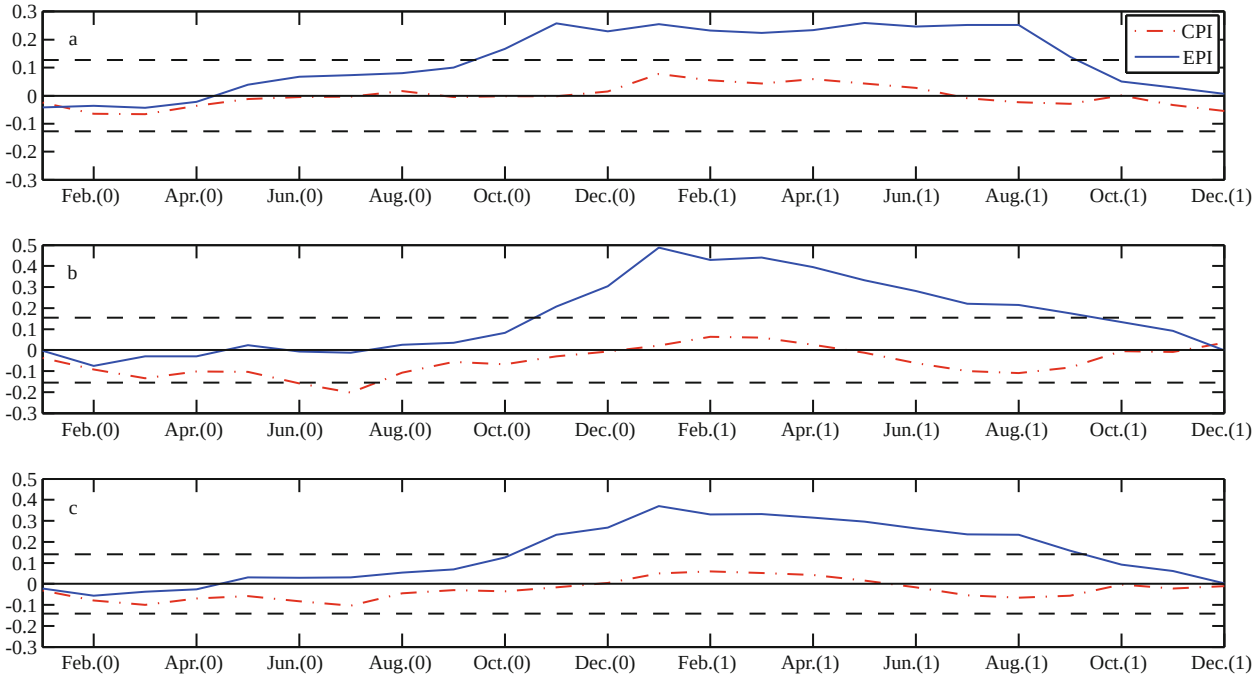

Fig.7 Time evolution of the regional average SST index in (a) North Indian Ocean, (b) South Indian Ocean and (c) the entire tropical Indian Ocean during EL, the blue solid lines for EPI-EL and the red dashed lines for CPI-El

Unit: °C.

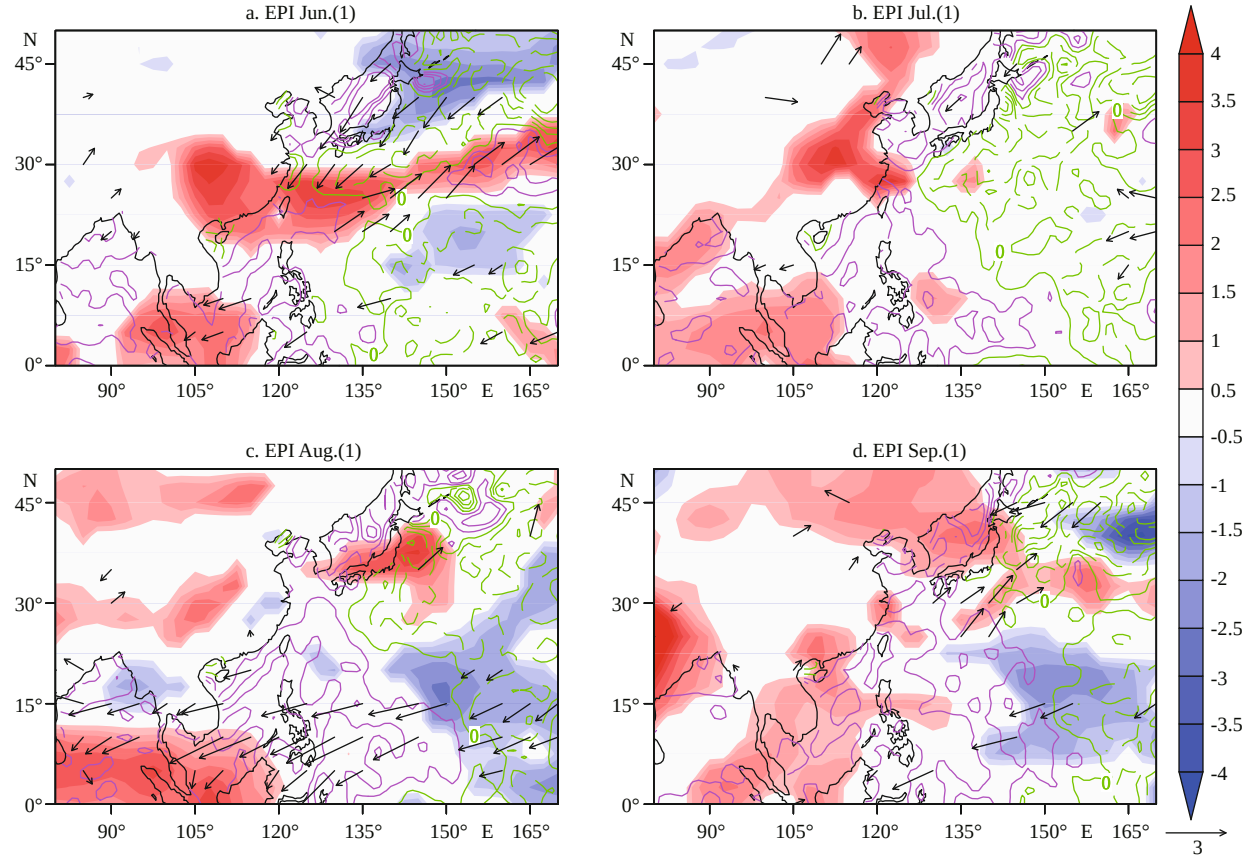

Fig.8 The Northwest Pacific SST anomaly (contour lines, red for positive anomalies and green for negative anomalies, interval is 0.2°C), sea surface wind anomalies (95% *t*-test, 3 m/s), convective precipitation anomalies (95% *t*-test, kg/m²) from June to September during the EPI-EL

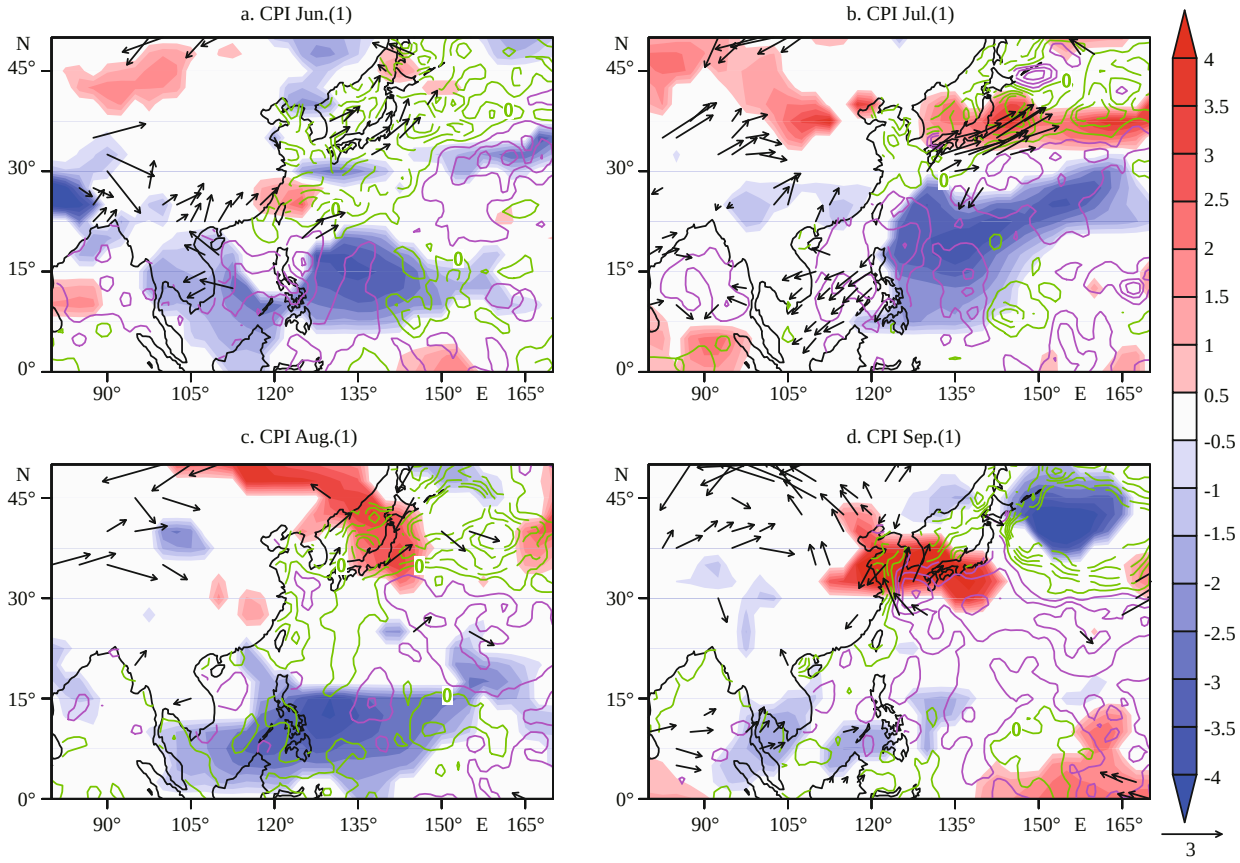

Fig.9 The Northwest Pacific SST anomaly (contour lines, red for positive anomalies and green for negative anomalies, interval is 0.2°C), sea surface wind anomalies (95% *t*-test, 3 m/s), convective precipitation anomalies (95% *t*-test, kg/m^2) from June to September during the CPI-EL

significant northeasterly and anticyclonic anomalies exist over between the tropical Indian and Pacific Oceans. Also in the Aug(0), there is a wide range of positive rainfall anomalies over the tropical Indian Ocean, while negative rainfall anomalies exist over the Northwest Pacific. In the case of CPI-EL, there are no sustained SST and wind anomalies in Northwest Pacific. But as can be seen, the negative rainfall anomalies in the Northwest Pacific appears in Jun(0) (Fig.9). Considering the time evolution of the North Indian Ocean warm SST anomaly (Fig.7a), we find that stronger warm SST anomaly exists in Indian Ocean from summer to autumn for EPI-EL decaying year, with significant zonal temperature gradient, and anticyclonic atmospheric circulation anomaly in the Northwest Pacific. In the case of CPI-EL, the positive SST anomaly in North Indian is weak and can only maintain to Jul(0) (Fig.7a), with weak northeasterly sea surface wind anomaly in the Northwest Pacific during Jun(0) and Jul(0).

It has been proved that the positive feedback mechanism between the Northwest Pacific cold SST anomaly and local wind fields during EL (Wang et al., 2000), the relationship between solar shortwave radiation and local atmospheric convective inhibition (Wu et al., 2010) and the Wind-Evaporation-SST (WES) positive feedback caused by the Northwest zonal SST gradient (Xie et al., 1994; Hu et al., 2011) are closely associated with the inter-annual variation of summer rainfall in East Asia. Figure 10 shows the evolution characteristics of the Northwest Pacific rainfall, anticyclonic atmospheric circulation and the Northwest Pacific SST anomaly in the EPI- and CPI-ELs. As can be seen from the figure, they are distinct in these two types of EL, especially in the decaying year of EL. In the evolution of the Northwest Pacific zonal SST gradient (Fig.10a), there are warm SST anomaly in the west but cold SST anomaly in the east of Northwest Pacific for EPI-EL. However, in the CPI-EL, the results are just the opposite. In the EPI-EL decaying summer, the dipole (warm in the west and cold in the east) type SST anomaly is advantageous to the anticyclonic circulation and negative precipitation anomalies. Hu et al. (2011, 2013a)

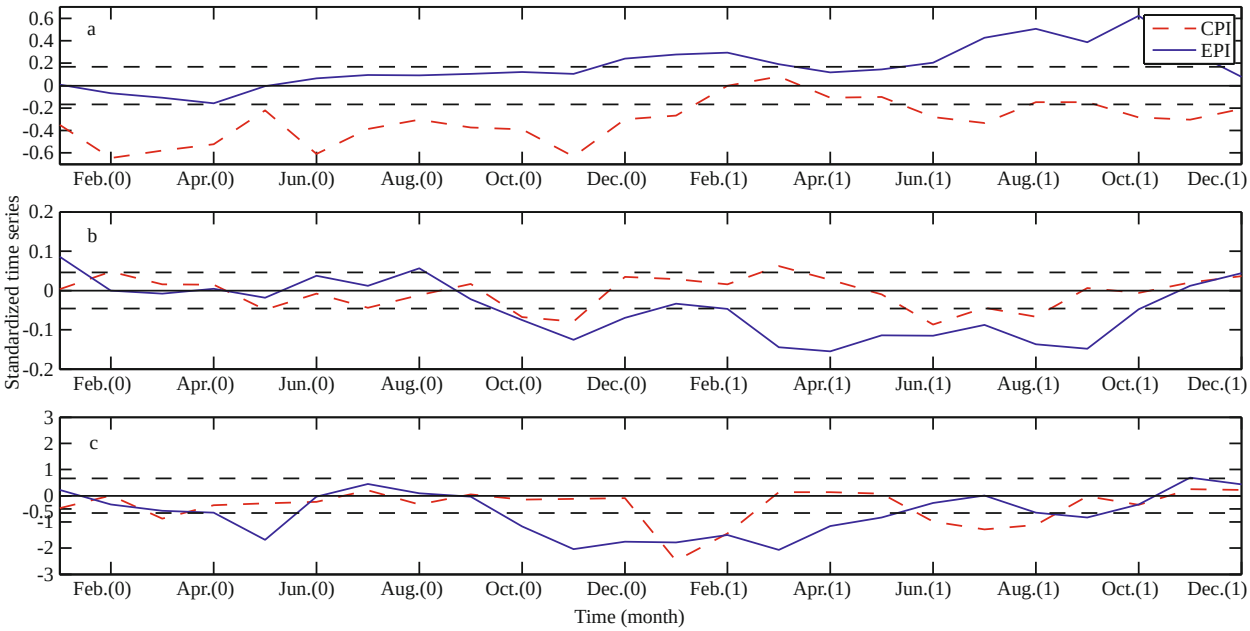

Fig.10 Time evolution characteristics of (a) average sea temperature difference between Northwest Pacific west region (125°–145°E, 4°–20°N) and east region (145°–170°E, 4°–20°N), (b) anticyclonic vortex index of Northwest Pacific (125°–147.5°E, 10°–25°N) and (c) rainfall anomalies in the Northwest Pacific anticyclone region during EL

The blue solid lines for EPI-EL and the red dashed lines for CPI-EL.

pointed out that on the background of South Asian monsoon, the warm SST anomaly over Indian Ocean led to significant positive precipitation anomalies and heated the lower level atmosphere. The atmospheric Kelvin wave then inspired, and propagated eastward with easterly wind anomalies. Then it weakened the sea surface wind over the west region of Northwest Pacific, but enhanced the east one. Because of the WES positive mechanism, the local anticyclone atmospheric circulation anomaly generates and suppresses the atmospheric convection. Therefore, the differences of the zonal sea surface temperature gradient in Northwest Pacific are likely caused by the different North Indian warming performances for two types of EL. It is the very evolution of zonal SST gradient that leads to the "secondary enhancement" phenomenon of the Northwest anticyclone and negative rainfall anomalies, which can be maintained until late autumn of EL decaying year (Fig.10b, c). In Jun(0) to Aug(0) of CPI-EL, there is only a weak anticyclonic circulation and negative precipitation anomaly over Northwest Pacific, but these anomalies decay rapidly after Aug(0). The Indian warm SST anomaly during Jun(0) to Jul(0) of CPI-EL (Fig.7a) and the positive rainfall anomaly (Fig.9b) in North Indian Ocean are the main reasons why the Northwest Pacific anticyclone generates in this time and inhibits the convection.

4 SUMMARY AND DISCUSSION

In this paper, we used HadISST1 assimilating sea surface temperature data and NCEP assimilating atmospheric field datasets to compare the effects of the two types of El Niño events (EP- and CP-ELs) on the tropical Indian Ocean SST anomaly, and then discussed the specific differences of the Northwest Pacific ocean-atmosphere coupling system between the two types of EL. In order to better reflect the impacts of ELs on the India Ocean SST anomaly, we set the threshold of ENSO episodes as the Niño index exceeding its 0.75 standard deviation for 5 consecutive months, which is different from Kao and Yu (2009). As can be seen from the synthesis analysis, in autumn of EP-EL developing year, it's more conducive to the development of the east equatorial Indian Ocean cold SST anomaly and ultimately leads to the Indian Ocean Dipole (IOD) event. By contrast, the IOD positive phase is advantageous to the enhancing of west wind anomalies over the eastern Northwest Pacific. What's more, the ocean warm advection and the eastward Kelvin wave also help to the development of warm SST anomaly in equatorial Pacific during EL. Basin uniform warm SST anomalies exist in the Indian Ocean in the whole summer of EL decaying year for both CP- and EP-ELs. However, considering the significance, more significant warm SST anomalies

only appear in the North Indian Ocean among the June and August of EP-EL decaying year.

The remote forcing mechanism of Indian Ocean warm SST anomaly, the positive feedback mechanism between the Northwest Pacific cold SST anomaly and the local Northwest Pacific anticyclonic circulation anomaly are very important for the summer precipitation in the East Asia. In order to better distinguish the differences of Indian Ocean SST anomaly for two types of EL, especially the different effects on the Northwest Pacific, we further define the EPI-EL (EP-EL with IOB event) and CPI-EL (CP-EL with IOB event). They are defined as the cases that maintain Indian Ocean warming in the decaying year of two types of EL. In the EPI- and CPI-ELs, warm SST anomalies appear in Indian Ocean, especially in the North Indian Ocean from May of EL developing year and persist to the EL decaying year. The persistence warming of North Indian Ocean during the EPI-EL is more significant, and maintains until the EL decaying autumn. As for the CPI-EL, the warm SST anomaly in the North Indian Ocean is weaker and can only persist to the July of EL developing year. Corresponding to the differences of the warm SST anomaly in the North Indian Ocean, the Northwest Pacific zonal sea surface temperature gradients of both ELs have significant differences. Using the 145°E as the boundary, there are zonal SST gradient anomaly (warm SST anomaly in the west but cold SST anomaly in the east), significant atmospheric anticyclonic circulation and the negative precipitation anomaly in the EPI-EL decaying summer. However, a weak reverse SST gradient anomaly exists during the CPI-EL. The warm North Indian SST anomaly persists until the August of the EPI-EL developing year. Considering the South Asian Summer Monsoon, this warm SST anomaly leads to a significant positive precipitation anomaly and heats the troposphere over the Northwest Pacific. The atmospheric Kelvin wave then inspires and propagates eastward with easterly wind anomalies. It weakens the sea surface wind over the western region of the Northwest Pacific, but enhances the eastern one. During the June and July of CPI-EL developing year, only a weak anticyclonic circulation and negative precipitation anomalies generate, but these anomalies decay rapidly after August in the EL developing year.

However, there are still controversies about the classification of ENSO events and their generation mechanism with the climate change (Choi et al., 2012; Xiang et al., 2012). Besides, Guo et al. (2015) found three types of IOD according to their relation with EL using CMIP5 datasets, which is not discussed in this paper now. In addition, the current conclusions are only suitable for the El Niño events, it yet to be determined when the La Niña events occur in the tropical Pacific.

5 ACKNOWLEDGEMENT

The authors would appreciate two anonymous reviewers for their constructive comments and suggestions to improve the manuscript. This work has benefited from discussions with Prof. Willam Perrie of BIO. Thanks to the support of the Jiangsu provincial Innovation Center for climate change.

References

Annamalai H, Murtugudde R, Potemra J et al. 2003. Coupled dynamics over the Indian Ocean: Spring initiation of the zonal mode. *Deep Sea Res. Part II Top Stud Oceanogr.*, **50**(12-13): 2 305-2 330.

Annamalai H, Xie S P, McCreary J P et al. 2005. Impact of indian ocean sea surface temperature on developing El Niño. *J. Climate*, **18**(2): 302-319.

Ashok K, Behera S K, Rao S A et al. 2007. El Niño modoki and its possible teleconnection. *J. Geophys. Res.*, **112**(C11): C11007.

Choi J, An S I, Yeh S W et al. 2012. ENSO-like and ENSO-induced tropical Pacific decadal variability in CGCMs. *J. Climate*, **26**(5): 1 485-1 501.

Du Y, Xie S P, Huang G et al. 2009. Role of air-sea interaction in the long persistence of El Niño-induced North Indian Ocean warming. *J. Climate*, **22**(8): 2 023-2 038.

Du Y, Yang L, Xie S P. 2011. Tropical Indian ocean influence on northwest pacific tropical cyclones in summer following strong El Niño. *J. Climate*, **24**(1): 315-322.

Fan L, Shin S I, Liu Q Y et al. 2013. Relative importance of tropical SST anomalies in forcing East Asian summer monsoon circulation. *Geophys. Res. Lett.*, **40**(10): 2 471-2 477.

Feng J, Chen W, Tam C Y et al. 2011. Different impacts of El Niño and El Niño modoki on China rainfall in the decaying phases. *Int. J. Climatol.*, **31**(14)**:** 2 091-2 101.

Feng J, Li J P. 2011. Influence of El Niño modoki on spring rainfall over south China. *J. Geophys. Res.*, **116**(D13): D13102.

Feng J, Wang L, Chen W et al. 2010. Different impacts of two types of Pacific Ocean warming on southeast Asian rainfall during boreal winter. *J. Geophys. Res.*, **115**(D24): D24122.

Fu C B, Fletcher J. 1985. Two types of tropical warming event during EL Niño. *Chinese Science Bulletin*, **31**(8): 38-41.

Guo F Y, Liu Q Y, Sun S et al. 2015. Three types of Indian Ocean dipoles. *J. Climate*, **28**(8): 3 073-3 092.

Hu H B, He J, Wu Q G, Zhang Y. 2011. The Indian Ocean's

asymmetric effect on the coupling of the Northwest Pacific SST and anticyclone anomalies during its spring-summer transition after El Niño. *J. Oceanogr*., **67**(3): 315-321.

Hu H B, Hong X Y, Zhang Y et al. 2013a. The critical role of Indian summer monsoon on the remote forcing between Indian and Northwest Pacific during El Niño decaying year. *Sci. China Earth Sci*., **56**(3): 408-417.

Hu H B, Hong X Y, Zhang Y et al. 2013b. Remote forcing of Indian Ocean warming on Northwest Pacific during El Niño decaying years: a FOAM model approach. *Chin. J. Oceanol. Limnol*., **31**(6): 1 375-1 383, https://doi.org/10.1007/s00343-013-3075-1.

Huang G, Hu K M, Xie S P. 2010. Strengthening of tropical Indian Ocean teleconnection to the Northwest Pacific since the Mid-1970s: an atmospheric GCM study. *J. Climate*, **23**(19): 5 294-5 304.

Kao H Y, Yu J Y. 2009. Contrasting eastern-pacific and central-pacific types of El Niño. *J. Climate*, **22**(3): 615-632.

Klein S A, Soden B J, Lau N C. 1999. Remote sea surface temperature variations during ENSO: evidence for a tropical atmospheric bridge. *J. Climate*, **12**(4): 917-932.

Kug J S, Jin F F, An S I. 2009. Two types of El Niño events: cold tongue El Niño and warm pool El Niño. *J. Climate*, **22**(6): 1 499-1 515.

Larkin N K, Harrison D E. 2005. On the definition of El Niño and associated seasonal average U.S. weather anomalies. *Geophys. Res. Lett*., **32**(13): L13705.

McPhaden M J, Busalacchi A J, Cheney R et al. 1998. The tropical ocean-global atmosphere observing system: a decade of progress. *J. Geophys. Res*., **103**(C7): 14 169-14 240.

McPhaden M J, Lee T, McClurg D. 2011. El Niño and its relationship to changing background conditions in the tropical Pacific Ocean. *Geophys. Res. Lett*., **38**(15): L15709.

Murtugudde R, McCreary J P Jr, Busalacchi A J. 2000. Oceanic processes associated with anomalous events in the Indian Ocean with relevance to 1997-1998. *J. Geophys. Res*., **105**(C2): 3 295-3 306.

Nagura M, Konda M. 2007. The seasonal development of an SST anomaly in the Indian Ocean and its relationship to ENSO. *J. Climate*, **20**(1): 38-52.

Peng J B, Zhang Q Y, Chen L T. 2011. Connections between different types of El Niño and Southern/Northern Oscillation. *Acta Meteor. Sinica*, **25**(4): 506-516.

Rasmusson E M, Carpenter T H. 1982. Variations in tropical sea surface temperature and surface wind fields associated with the Southern Oscillation/El Niño. *Mon. Wea. Rev*., **110**(5): 354-384.

Ren H L, Jin F F. 2011. Niño indices for two types of ENSO. *Geophys Res Lett*, **38**(4): L04704.

Rong X Y, Zhang R H, Li T. 2010. Impacts of Atlantic sea surface temperature anomalies on Indo-East Asian summer monsoon-ENSO relationship. *Chin. Sci. Bull*., **55**(22): 2 458-2 468.

Roxy M, Gualdi S, Drbohlav H K L et al. 2011. Seasonality in the relationship between El Niño and Indian Ocean dipole. *Climate Dyn*., **37**(1-2): 221-236.

Saji N H, Goswami B N, Vinayachandran P N et al. 1999. A dipole mode in the tropical Indian Ocean. *Nature*, **401**(6751): 360-363.

Tan Y K, Zhang R H, He J H et al. 2004. Relationship of the interannual variations of sea surface temperature in tropical Indian ocean to ENSO. *Acta Meteorologica Sinica*, **62**(6): 831-840. (in Chinese)

Trenberth K E, Tepaniak D P. 2001. Indices of El Niño Evolution. *J Climate*, **14**(8): 1 697-1 701.

Wallace J M, Rasmusson E M, Mitchell T P et al. 1998. On the structure and evolution of ENSO-related climate variability in the tropical Pacific: lessons from TOGA. *J. Geophys. Res*., **103**(C7): 14 241-14 259.

Wang B, Wu R G, Fu X H. 2000. Pacific–East Asian teleconnection: how does ENSO affect East Asian climate?. *J. Climate*, **13**(9): 1 517-1 536.

Wang C Z, Wang X. 2013a. Classifying El Niño modoki I and II by different impacts on rainfall in southern China and typhoon tracks. *J. Climate*, **26**(4): 1 322-1 338.

Wang X, Wang C Z. 2013b. Different impacts of various El Niño events on the Indian Ocean Dipole. *Climate Dyn*., **42**(3-4): 991-1 005.

Wang X, Zhou W, Li C Y et al. 2014. Comparison of the impact of two types of El Niño on tropical cyclone genesis over the South China Sea. *Int. J. Climatol*., **34**(8): 2 651-2 660, doi: 10.1002/joc.3865.

Weng H Y, Ashok K, Behera S K et al. 2007. Impacts of recent El Niño modoki on dry/wet conditions in the Pacific Rim during boreal summer. *Climate Dyn*., **29**(2-3): 113-129.

Weng H Y, Wu G X, Liu Y M et al. 2011. Anomalous summer climate in China influenced by the tropical Indo-Pacific Oceans. *Climate Dyn*., **36**(3-4): 769-782.

Wu B, Tim L, Zhou T J. 2010. Relative contributions of the Indian Ocean and local SST anomalies to the maintenance of the Western North Pacific anomalous anticyclone during the El Niño decaying summer. *J. Climate*, **23**(11): 2 974-2 986.

Wu G X, Meng W. 1998. Gearing between the Indo-monsoon circulation and the Pacific-Walker circulation and the ENSO. Part I: data analyses. *Chinese Journal of Atmospheric Sciences*, **24**(1): 15-25. (in Chinese)

Wu R G, Kirtman B P. 2004. Understanding the impacts of the Indian Ocean on ENSO variability in a coupled GCM. *J. Climate*, **17**(20): 4 019-4 031.

Xiang B, Wang B, Ding Q et al. 2012. Reduction of the thermocline feedback associated with mean SST bias in ENSO simulation. *Climate Dynamics*, **39**(6): 1 413-1 430.

Xiao Y, Zhang Z Q, He J H. 2009. Progresses in the studies on Indian ocean dipoles. *Journal of Tropical Meteorology*, **25**(5): 621-627. (in Chinese)

Xie S P, Hu K M, Hafner J et al. 2009. Indian ocean capacitor effect on indo-western Pacific Climate during the Summer following El Niño. *J. Climate*, **22**(3): 730-747.

Xie S P, Philander S G H. 1994. A coupled ocean-atmosphere model of relevance to the ITCZ in the Eastern Pacific.

Tellus A, **46**(4): 340-350.

Xu K, Zhu C W, He J H. 2012. Linkage between the dominant modes in Pacific subsurface ocean temperature and the two type ENSO events. *Chin. Sci. Bull.*, **57**(26): 3 491-3 496.

Yang J L, Liu Q Y, Xie S P et al. 2007. Impact of the Indian Ocean SST basin mode on the Asian summer monsoon. *Geophys. Res. Lett.*, **34**(2): L02708.

Yeh S W, Kug J S, Dewitte B et al. 2009. El Niño in a changing climate. *Nature*, **461**(7263): 511-514.

Yu J Y, Kao H Y. 2007. Decadal changes of ENSO persistence barrier in SST and ocean heat content indices: 1958-2001. *J. Geophys. Res.*, **112**(D13): D13106.

Yu J Y, Kim S T. 2011. Relationships between extratropical sea level pressure variations and the central Pacific and eastern Pacific types of ENSO. *J. Climate*, **24**(3): 708-720.

Yuan Y, Yan H M. 2013. Different types of La Niña events and different responses of the tropical atmosphere. *Chin. Sci. Bull.*, **58**(3): 406-415.

Yuan Y, Yang S, Zhang Z Q. 2012. Different evolutions of the philippine sea anticyclone between the eastern and central Pacific El Niño: possible effects of Indian ocean SST. *J. Climate*, **25**(22): 7 867-7 883.

Yuan Y, Yang S. 2012. Impacts of different types of El Niño on the East Asian climate: focus on ENSO cycles. *J. Climate*, **25**(21): 7 702-7 722.

Zhang R H. 1999. The role of Indian summer Monsoon water vapor transportation on the summer rainfall anomalies in the northern part of China during the El Niño mature phase. *Plateau Meterology*, **18**(4): 567-574. (in Chinese)

Zhang W J, Jin F F, Li J P et al. 2011. Contrasting impacts of two-type El Niño over the western north Pacific during Boreal Autumn. *J. Meteor. Soc. Japan*, **89**(5): 563-569.

Zhao S S, Yang X Q. 2004. Numerical experiments on interaction between the tropical Pacific and the Indian Ocean through the wind-stress “bridge”. *Acta Oceanologica Sinica*, **26**(4): 33-48. (in Chinese)